

Design and Implementation of PRCC Based Solar Maximum Power Point Tracking System with Wind Energy Generation

^[1]Sangeet Gharai, ^[2]J.Ajay Daniel, ^[3]A. Nikhil

^{[1][3]}Student,; ^[2]Assistant Professor

^{[1][2][3]} Department of Electrical & Electronics Engineering, SRM University, Chennai.

^[1]gharai.sangeet@gmail.com, ^[2]ajaydaniel23@gmail.com, ^[3]anumolunikhil@gmail.com

Abstract: Demand for more energy makes us seek more energy resources. Now a days, solar and wind are the primary sources of renewable energy. But when they are used individually achieving uninterrupted power supply is difficult. Thus, the recent trends are moving towards the use of hybrid sources of energy. But still, the hybrid wind and solar energy model fails to achieve the expected efficiency because of the presence of natural and conversional ripples in the output current. This paper deals with the passive ripple cancellation circuit (PRCC) to reduce the amount of ripples produced in the output power obtained from wind and solar hybrid converters. Some of the special characteristics of the proposed PRCC model comprises of cheap, compact and adaptive structure that doesn't need any extra control and feedback circuit. Thus the ripples in the input current are eliminated by incorporating the proposed model into the main power circuit. Consequently, reduction in filter size is achieved with faster response. In the interim, the instantaneous tracking response is acquired by incorporating the continuous MPPT control with the proposed module integrated converter (MIC).

Index terms-- ĉuk- type Converter, Hybrid energy system, Maximum Power Point Tracking (MPPT), Module Integrated Converter (MIC), Passive Ripple Cancellation Circuit (PRCC), Photo voltaic module (PV), Wind energy system.

I. INTRODUCTION

Since the discovery of electricity the demand for electricity is increasing with each passing day. Initially, the non-renewable resources like coal, diesel etc. were used extensively for electricity generation. The non-renewable energy usage has come to a point where exploration of alternative energy resources is necessary. Now a days, solar and wind are the primary sources of renewable energy [1],[2].The conversion of sunlight into electricity using photoelectric effect is known as solar power[3]. Solar energy has proved to be a cost-effective and reliable source of energy. The latest technology in the field of solar energy has led it into becoming the major force among all the available non-conventional sources of energy[3],[4].Wind energy is also one of the upcoming non-traditional sources of energy that has shown a promising future in yielding efficient green energy[5]-[7]. The kinetic energy of wind can be harnessed and redirected to generate electrical power[7].Although solar and wind energy conversion systems are effective individually, the seasonal and daily variations result in the generation of just a passable output[2]. So, it is requisitory to focus on the extraction of more energy from both solar and wind energy [9]. By adapting a hybrid energy system of both the afore mentioned energies will not only overcome the

disadvantages of the individual system but also achieve effective output[8],[9]. The use of hybrid solar-wind substantially optimizes the power generation and reliability of those systems[10].Since the beginning of usage of non-conventional energy systems, the energy obtained has been consistently marred with losses because of natural and conventional ripple present in the output[11]-[13]. To solve the above problem, a ripple filter is installed which is a parallel combination of bulky capacitor, power converters and PV module. This model is not only bulky but also reduces the lifespan of power converters [21]. A ripple filter can be integrated into converter to reduce the amount of ripple produced [14] -[20]. However, this method is sensitive to the k coefficient of coupling due to integrated magnetic component[21]. So, in this paper a conventional ĉuk type converter is integrated with an isolating transformer so as to obtain a non-pulsating input/output current feature and step up/ step down capability. The main objective of the paper is to improve the efficiency of the system by reducing the natural input current ripple produced by the photovoltaic module and the conversional output current ripple generated by the wind turbine setup by proposing a passive ripple cancellation technique to overcome the above issues.

II. PROPOSED MODEL

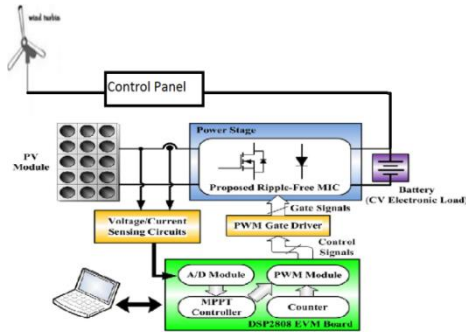


Fig. 1 Proposed model of PRCC based maximum power point tracking system with wind energy generation.

The proposed PRCC are integrated into the input side of a conventional ĉuk-type converter to eliminate the input current ripple. It turns out that the more precise MPPT control of the proposed MIC for PV energy harvesting can now be achieved easily. Solar radiation can be converted directly or indirectly into heat or electricity. This radiation in the form of electromagnetic waves mostly have wavelength of 0.2 to 4 micro meter. The output from the solar is a direct current.

$$I_{pv} = I_s - I_o \left[e^{\frac{V_{pv} + I_{pv} R_s}{\alpha}} - 1 \right]$$

$$\alpha = \frac{AKT}{q}$$

Where,
 I_s = Generated current under a given irradiance value
 I_o = Reverse saturation current
 q = Charge of an electron
 K = Boltzmann's constant
 T = Temperature
 A = Diode ideality constant
 α = Photovoltaic constant

In this proposed model hybrid solar and wind energy is utilised to achieve efficient output. Wind power generators convert wind energy (mechanical energy) into electrical energy. The relation between wind velocity and the power generated by the wind is given below:

$$\frac{P}{m^2} = 6.1 \times 10^{-4} * V^3$$

Where, P- Power of wind
V- Wind velocity
m- Mass of wind

The wind turbine generates alternating current which also has a converter, periodically converting the AC to DC using rectifier thereby reversing the direction.

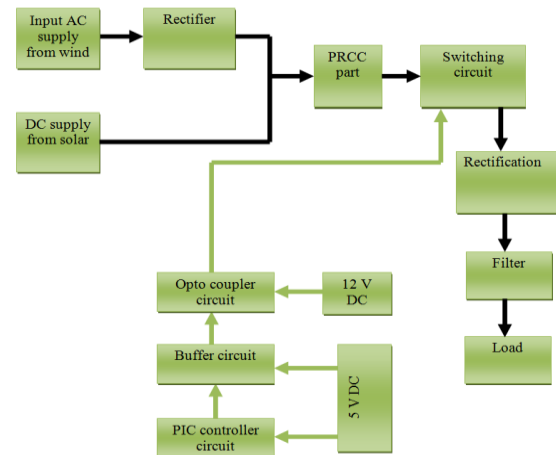


Fig. 2 Block diagram of proposed PRCC

The PRCC part consists of passive ripple cancellation circuit that is majorly responsible for reducing the amount of natural and conversional ripples, present in the current obtained from hybrid solar and wind energy respectively, to zero. The PRCC model comprises of a magnetizing inductor and two blocking capacitors that contribute in magnetizing the input current for the PRCC. This magnetizing current is then processed through the isolating ideal transformer which is integrated into the converter. Once the above process is complete, the current passes through the ĉuk type converter so as to boost the amount of current generated originally. The operation of PRCC is complete here. The boosted and the ripple free current from the PRCC is sent to the switching circuit. The switching circuit also plays a vital role in the whole scheme of things. The MPPT feedback from the solar panel is controlled using a PIC controller circuit that is boosted up using a buffer circuit. The resulting signal is then used for the switching circuit. The switching circuit reduces the ripples left out in the pulsating DC from the rectifier. The opto-coupler is added to the circuit for the protection of controller circuit from different conversions occurring simultaneously in the operating circuit. The next stage of operation is a combination of rectifier and filter that does the final conversion of current so as to minimize the remaining ripples, if any. The final ripple free current is obtained in this step and sent to the load for further use.

III. CIRCUIT DIAGRAM AND OPERATION OF PRCC:

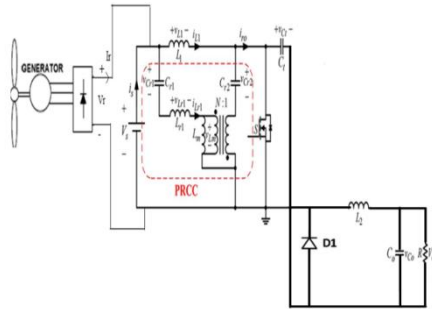


Fig. 3 Circuit diagram of PRCC model.

The parameters of the proposed MIC are listed in the table 1.

TABLE 1: Parameters of the proposed MIC:

Parameters	Values
Input/output Inductors(L1, L2)	200μH
Ripple mirror inductor(Lr1)	200μH
Turns ratio	1
Intermediate capacitor(C1)	60μF
Output filter capacitor(C0)	440μF
Blocking capacitor(Cr1,Cr2)	10μF

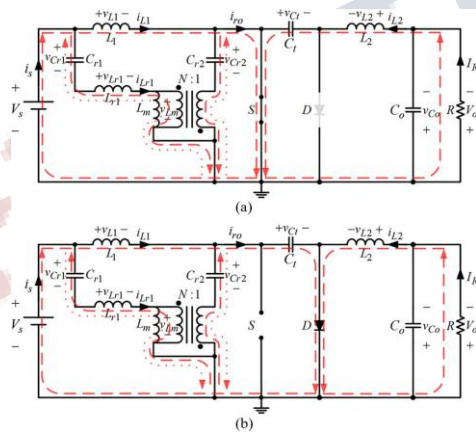


Fig. 4 Modes of operation of PRCC. (a) When the switch is ON, (b) When the switch is OFF

The circuit diagram explains the passive ripple cancellation circuit performing 2 modes of operation based on the position of MOSFET. The characteristics of power MOSFET includes lower switching losses, positive temperature coefficient of resistance thereby making an easy parallel MOSFET operation.

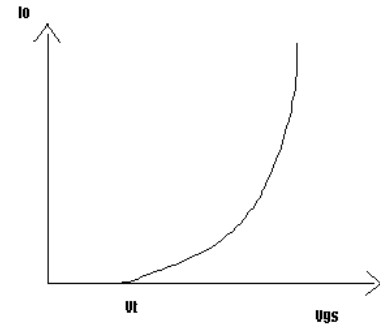


Fig. 5 Transfer characteristic of MOSFET

A. MODE 1(a):

In the first mode of operation, the MOSFET S is switched ON which reverses the diode D. Thus, the capacitor Ct is connected across the output and the energy is directly transferred from it to the combination of C2 and C0 filter. Thus, the output here is the charge present in the capacitor Ct.

B. MODE 2(b):

When the MOSFET S is switched off it leads to the second mode of operation. In this mode, the diode D is forward biased and the capacitor Ct is charged through diode. This capacitor even receives energy from source voltage Vs and inductor L1. Besides, the high frequency Alternative current of the inductor L1 is given back to the inductor Lr1 due to the blocking capacitors Cr1, Cr2 and the reverse polarity of the transformer. In order to get the required output the polarity can be changed accordingly.

IV. STAE DY STATE ANALYSIS OF PROPOSED MIC:

In solar PV module, the natural ripple causing the decreased output can be given as,

$$I_{pv} = I_s - I_0 \left[e^{\frac{V_{pv} + I_{pv} R_s}{\alpha}} - 1 \right] \quad (1)$$

$$\alpha = \frac{AKT}{q}$$

Where,

Is= Generated current under a given irradiance value

I0= Reverse saturation current

q = Charge of an electron

K= Boltzmann's constant

T= Temperature

A= Diode ideality constant

α=Photovoltaic constant

Output voltage of PV module can be given as,

$$V_{pv} = -I_{pv}R_s + \alpha \ln\left(\frac{I_s + I_o - I_{pv}}{I_o}\right) \quad (2)$$

Multiplying (1) and (2), we get,

$$P_{pv} = -I_{pv}^2 R_s + 2 I_{pv} \ln\left(\frac{I_s + I_o - I_{pv}}{I_o}\right) \quad (3)$$

Now in case of wind energy, after the ac power is generated from the wind mill, it is sent to the rectifier. The rectifier gives us an output of the following manner. It is noted that the dc voltage wave form is periodic over half of the input cycle. Hence, we write the Fourier Series expression for the output voltage as,

$$V_o = V_{oAv} + \sum_{n=1}^{\infty} [V_{an} \cos 2n\omega t + V_{bn} \sin 2n\omega t] \quad (4)$$

Where,

$$\begin{aligned} V_{oAv} &= \frac{1}{\pi} \int_{\alpha}^{\pi+\alpha} V_o d\omega t = \frac{2\sqrt{2}}{\pi} V_i \cos \alpha, \\ V_{an} &= \frac{2}{\pi} \int_0^{\pi} V_o \cos 2n\omega t d\omega t \\ &= \frac{2\sqrt{2}}{\pi} V_i \left[\frac{\cos(2n+1)\alpha}{2n+1} - \frac{\cos(2n-1)\alpha}{2n-1} \right], \\ V_{bn} &= \frac{2}{\pi} \int_0^{\pi} V_o \sin 2n\omega t d\omega t \\ &= \frac{2\sqrt{2}}{\pi} V_i \left[\frac{\sin(2n+1)\alpha}{2n+1} - \frac{\sin(2n-1)\alpha}{2n-1} \right]. \end{aligned}$$

Since, the voltage wave form is periodic; the current wave form is also periodic over an interval π . Therefore we choose an interval $\alpha \leq \omega t \leq \pi + \alpha$.

In this interval,

$$L \frac{di_o}{dt} + Ri_o + E = \sqrt{2}V_i \sin \omega t$$

After solving the above differential equation we obtain the general solution as,

$$i_o = I e^{-\frac{\omega t - \alpha}{\tan \varphi}} + \frac{\sqrt{2}V_i}{Z} \left[\sin(\omega t - \varphi) - \frac{\sin \theta}{\cos \varphi} \right]$$

$$\text{where } = \sqrt{R^2 + \omega^2 L^2}; \tan \varphi = \frac{\omega L}{R};$$

$$E = \sqrt{2}V_i \sin \theta; R = Z \cos \varphi$$

At steady state,

$$i_o|_{\omega t = \alpha} = i_o|_{\omega t = \pi + \alpha}$$

Output current will be,

$$i_o = \frac{\sqrt{2}V_i}{Z} \left[\frac{2 \sin(\varphi - \alpha)}{1 - e^{-\frac{\pi}{\tan \varphi}}} - \frac{(\omega t - \alpha)}{\tan \varphi} + \sin(\omega t - \varphi) - \frac{\sin \theta}{\cos \varphi} \right] \quad (5)$$

So, finally adding (2) and (4), the combined equation of voltage and current for solar and wind will be obtained.

$$V = V_o + V_{pv}$$

$$\begin{aligned} &= V_{oAv} + \sum_{n=1}^{\infty} [V_{an} \cos 2n\omega t + V_{bn} \sin 2n\omega t] - I_{pv}R_s \\ &\quad + \alpha I_{pv} \ln\left(\frac{I_s + I_o - I_{pv}}{I_o}\right) \end{aligned}$$

Adding (1) and (5),

$$\begin{aligned} I &= i_o + I_{pv} \\ &= I_s + I_o \left[e^{\frac{V_{pv} + I_{pv}R_s}{\alpha}} - 1 \right] + \frac{\sqrt{2}V_i}{Z} \left[\frac{2 \sin(\varphi - \alpha)}{1 - e^{-\frac{\pi}{\tan \varphi}}} e^{-\frac{(\omega t - \alpha)}{\tan \varphi}} + \sin(\omega t - \varphi) - \frac{\sin \theta}{\cos \varphi} \right] \end{aligned}$$

V. SIMULATION DIAGRAM:

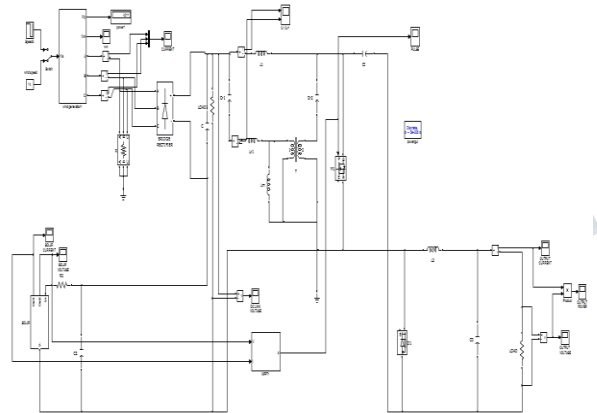


Fig. 6 The simulation circuit diagram of Current-Ripple-Free Module Integrated Converter With More Precise MPPT Control for PV Energy Harvesting and Wind Energy Generation

1. OUTPUT VOLTAGE:

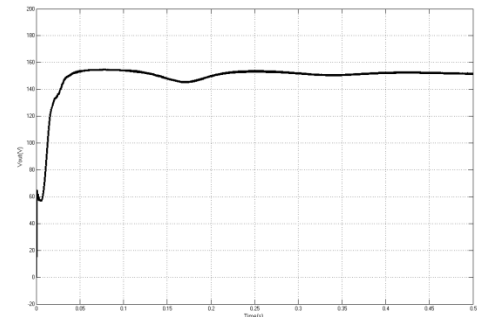


Fig. 7 The characteristics of output voltage for hybrid energy system.

The waveform shows the Output voltage of Current-Ripple-Free Module Integrated Converter With More Precise Maximum Power Tracking Control for PV Energy

Harvesting and wind energy. The output voltage of hybrid system is compared with the individual operation of solar and wind respectively. On noting the similarity, an improved output voltage is obtained in the proposed hybrid system. The output voltage for the proposed hybrid model is 155 V.

2. OUTPUT CURRENT:

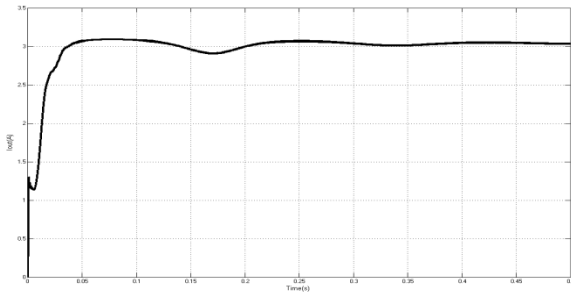


Fig. 8 The characteristics of output current for hybrid energy system.

The waveform shows the Output current of Current-Ripple-Free Module Integrated Converter With More Precise Maximum Power Tracking Control for PV Energy Harvesting and wind energy. On estimating the output current of wind, solar and hybrid energy system, the result is almost the same for the individual operation of wind and solar energy. But, the proposed hybrid system results in a massive growth in output current waveform. The value of output current is 3.1 A.

3. OUTPUT POWER:

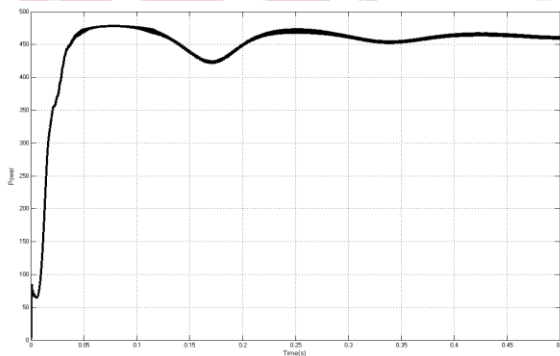


Fig. 9 The characteristics of output power for hybrid power system.

The waveform shows the Output power of Current-Ripple-Free Module Integrated Converter With More Precise Maximum Power Tracking Control for PV Energy Harvesting and wind energy. The progressive increase in the output voltage and current of the hybrid energy system

substantially increase the value of the output power. The output power for the hybrid model is 480 W. The comparative values of the output voltage, current and power are mentioned in the table 2.

TABLE2: Comparative values of output voltage, current and power

	SOLAR	WIND	HYBRID
Input voltage	56 V	62 v	48 v
Input current	3 A	3.5	8 A
Gate pulse	1 V	1 V	1 V
I_{L1}	45 A	50 A	50 A
I_{Lr1}	2 A	2 A	2.5 A
Output voltage	110 V	118 V	155 V
Output current	2.2 A	2.3 A	3.1 A
Output power	220 W	275 W	480 W

VII. CONCLUSION

This paper successfully proposes a cheap and simply designed Passive Ripple Cancellation Circuit that eliminates the current ripple from the conventional Ćuk type converter. Comparing the output of PV, wind and hybrid energy systems, we come to a conclusion that the hybrid solar- wind energy system is the most effective system at producing a substantial ripple free output. The effect of ripple cancellation circuit has given in table 3.

TABLE 3: Input current ripple Cancelling effects:

Input voltage (V_s)	Inductor ripple (Δi_{L1})	Input ripple (Δi_s)	Ripple cancelling ratio $\delta = 1 - (\Delta i_s / \Delta i_{L1})$
24 V	1.59 A	0.030 A	98.1%
26 V	1.60 A	0.035 A	97.8%
28 V	1.66 A	0.035 A	97.9%
30 V	1.70 A	0.037 A	97.8%
32 V	1.74 A	0.035 A	98.0%
34 V	1.78 A	0.040 A	97.8%

REFERENCES:

- 1) S. R. Bull, "Renewable energy today and tomorrow," Proc. IEEE, vol. 89, no. 8, pp. 1216–1226, Aug. 2001.
- 2) Eduardo F. Camacho, Tariq Samad, Mario Garcia-Sanz, and Ian Hiskens, "Control for Renewable Energy and Smart Grids," : The Impact of Control Technology, T. Samad and A.M. Annaswamy (eds.), 2011.
- 3) J. T. Bialasiewicz, "Renewable energy systems with photovoltaic powergenerators: Operation and modeling," IEEE Trans. Ind. Electron., vol. 55, no. 7, pp. 2752–2758, Jul. 2008.
- 4) E. V. Orosco, " Simulation results of an efficient and innovative sun engine for solar to electrical energy conversion," : Energy Conversion Engineering Conference and Exhibit, 2000. (IECEC) 35th Intersociety Page(s):908 - 914 vol.2 24 Jul 2000-28 Jul 2000
- 5) Ying Zuo and Hongyan Liu, " Evaluation on comprehensive benefit of wind power generation and utilization of wind energy,"
- 6) E. Lerch, " Storage of fluctuating wind energy," Power Electronics and Applications, 2007 European Conference, IEEE Page(s):1 - 8 2-5 Sept. 2007
- 7) T. Dai ; B. Song & S. W. Shu, " Study on the wind energy resources assessment in wind power generation," Artificial Intelligence, Management Science and Electronic Commerce (AIMSEC), 2011 2nd International Conference, IEEE 8-10 Aug. 2011 Page(s):6804 - 6807
- 8) PragmaNema, R.K. Nema&SarojRangnekar, " A current and future state of art development of hybrid energy system using wind and PV-solar: A review," Renewable and Sustainable Energy Reviews, Volume 13, Issue 8, October 2009, Pages 2096–2103
- 9) Wei Zhou, Chengzhi Lou, Zhongshi Li, Lin Lu&HongxingYang^a, " Current status of research on optimum sizing of stand-alone hybrid solar-wind power generation systems," Applied Energy, Volume 87, Issue 2, February 2010, Pages 380–389
- 10) K. Mousa, H. AlZu'bi&A. Diabat, " Current Model Design of a hybrid solar-wind power plant using optimization," Engineering Systems Management and Its Applications (ICESMA), 2010 Second International Conference Page(s):1 - 6
- 11) R. Billinton&Bagen, " Reliability Considerations in the Utilization of Wind Energy, Solar Energy and Energy Storage in Electric Power Systems," Probabilistic Methods Applied to Power Systems, 2006. PMAPS 2006. International Conference IEEE 11-15 June 2006 Page(s):1 - 6
- 12) Shin-Li Lin ; Gwo-Bin Wu ; Wei-Chen Liu ; Chin-Sien Moo, " Ripple current effect on output power of solar-cell panel," Renewable Energy Research and Applications (ICRERA), 2012 International Conference IEEE 11-14 Nov. 2012 Page(s):1 - 5
- 13) H. Hu, S. Harb, N. H. Kutkut, Z. J. Shen, and I. Batarseh, "A single-stage microinverter without using eletrolytic capacitors," IEEE Trans. PowerElectron., vol. 28, no. 6, pp. 2677–2687, Jun. 2013.
- 14) S. C' uk, "A new zero-ripple switching DC-to-DC converter and integrated magnetics," IEEE Trans. Magn., vol. MAG-19, no. 2, pp. 57–75, Mar. 1983.
- 15) J. Wang, W. G. Dunford, and K. Mauch, "Analysis of a ripple-free input current boost converter with discontinuous conduction characteristics," IEEE Trans. Power Electron., vol. 12, no. 4, pp. 684–694, Jul. 1997.
- 16) G. Zhu, B. McDonald, and K. Wang, "Modeling and analysis of coupled inductors in power converters," in Proc. IEEE Appl. Power Electron. Conf.Expo. Conf., Feb. 2009, pp. 83–89.
- 17) J. Wang, W. G. Dunford, and K. Mauch, "Design of zero-current switching fixed frequency boost and buck converters with coupled inductors," in Proc. IEEE PESC, Jun. 1995, vol. 1, pp. 273–279.
- 18) D. C. Hamill and P. T. Krein, "A 'Zero' ripple technique applicable to any DC converter," in Proc. IEEE PESC, Jul. 1999, pp. 1165–1171.
- 19) "Coupled-magnetic filters with adaptive inductance cancellation," in Proc. IEEE PESC, Jun. 2005, pp. 590–600.
- 20) M. J. Schutten, R. L. Steiqerwald, and J. A. Sabate, "Ripple current cancellation circuit," in Proc. IEEE Appl. Power Electron. Conf. Expo., Feb. 2003, vol. 1, pp. 464–470.
- 21) Ching-Tsai Pan, Ming-Chieh Cheng, Ching-Ming Lai and Po-Yen Chen, " Current-Ripple-Free Module Integrated Converter With More Precise Maximum Power Tracking Control for PV Energy Harvesting," IEEE TRANSACTIONS ON INDUSTRY APPLICATIONS, VOL. 51, NO. 1, JANUARY/FEBRUARY 2015 pp. 271-278